Brain (1998), **121,** 1513–1531

Functional coupling and regional activation of human cortical motor areas during simple, internally paced and externally paced finger movements

Christian Gerloff, Jacob Richard, Jordan Hadley, Andrew E. Schulman, Manabu Honda and Mark Hallett

Human Motor Control Section, Medical Neurology Branch, National Institute of Neurological Disorders and Stroke, National Institutes of Health, Bethesda, Maryland, USA

Correspondence to: Christian Gerloff, Building 10, Room 5N226, NINDS, NIH, 10 Center Drive, MSC-1428, Bethesda, MD 20892-1428, USA

Summary

We studied the activation and interaction of cortical motor regions during simple, internally paced and externally paced right-hand finger extensions in healthy volunteers. We recorded EEGs from 28 scalp electrodes and analysed task-related coherence, task-related power and movement-related cortical potentials. Task-related coherence reflects inter-regional functional coupling of oscillatory neuronal activity, task-related power reflects regional oscillatory activity of neuronal assemblies and movement-related cortical potentials reflect summated potentials of apical dendrites of pyramidal cells. A combination of these three analytical techniques allows comprehensive evaluation of different aspects of information processing in neuronal assemblies. For both externally and internally paced finger extensions, movement-related regional activation was predominant over the contralateral premotor and primary sensorimotor cortex, and functional coupling occurred between the primary sensorimotor cortex of both hemispheres and between the primary sensorimotor cortex and the mesial premotor areas, probably including the supplementary motor area. The main difference between the different types of movement pacing was enhanced functional coupling of central motor areas during internally paced finger extensions, particularly inter-hemispherically between the left and right primary sensorimotor cortexes and between the contralateral primary sensorimotor cortex and the mesial premotor areas. Internally paced finger extensions were also associated with additional regional (premovement) activation over the mesial premotor areas. The maximal task-related coherence differences between internally and externally paced finger extensions occurred in the frequency range of 20–22 Hz rather than in the range of maximal task-related power differences (9–11 Hz). This suggests that important aspects of information processing in the human motor system could be based on network-like oscillatory cortical activity and might be modulated on at least two levels, which to some extent can operate independently from each other: (i) regional activation (task-related power) and (ii) inter-regional functional coupling. We propose that internal pacing of movement poses higher demands on the motor system than external pacing, and that the motor system responds not only by increasing regional activation of the mesial premotor system, including the supplementary motor area, but also by enhancing information flow between lateral and mesial premotor and sensorimotor areas of both hemispheres, even if the movements are simple and unimanual.

Keywords: motor cortex; supplementary motor area; finger movements; EEG; motor control

Abbreviations: ANOVA = analysis of variance; EOI = electrode of interest; MRCP = movement-related cortical potential; POI = electrode pair of interest; SMA = supplementary motor area; SM1 = primary sensorimotor area

Introduction

Internally generated and externally triggered movements are associated with different cortical activation patterns (Kurata and Wise, 1988; Mushiake *et al.*, 1991; Halsband *et al.*, 1993, 1994; Jahanshahi *et al.*, 1995; Deiber *et al.*, 1996; Picard and Strick, 1996*a*, *b*; Wessel *et al.*, 1997). Internal generation and external triggering can refer to various aspects of movement (e.g. timing, movement selection). In the present study we focused on brain activation during internal and

external 'pacing', i.e. during the absence and presence of an external pacemaker (e.g. a metronome) serving to guide rhythmic movements.

Data on cortical activation patterns associated with internal and external pacing of rhythmic movement are sparse and contradictory (Rao *et al.*, 1993; Remy *et al.*, 1994; Jahanshahi *et al.*, 1995). Previous studies in non-human primates have suggested that the supplementary motor area (SMA) is particularly involved with internally generated movements (Kurata and Wise, 1988; Mushiake *et al.*, 1991; Halsband *et al.*, 1994). This view gains support from clinical observations in patients with Parkinson's disease and dysfunction of the mesial premotor system (Marsden, 1989; Hallett, 1990; Jenkins *et al.*, 1992; Playford *et al.*, 1992; Rascol *et al.*, 1993, 1994), and in patients with structural lesions of the SMA (Halsband *et al.*, 1993). Microelectrode recordings in monkeys (Tanji, 1994; Shima *et al.*, 1996; Tanji and Shima, 1996), however, indicate that the SMA is not exclusively concerned with internally generated movements but is also concerned with externally triggered movements (Tanji and Shima, 1996). A possible reason for some inconsistencies among previous results is that the motor system may not implement internally generated and externally triggered movements by the use of one or another cortical region exclusively, but rather by dynamically modulating the activity in a cortical network that integrates multiple regions including the primary sensorimotor area (SM1), lateral premotor cortex and SMA. Previous studies have focused on patterns of regional activation in association with internally generated and externally triggered movements using measurements of regional cerebral blood flow in humans (Jenkins *et al.*, 1992; Playford *et al.*, 1992; Rascol *et al.*, 1992, 1993, 1994; Rao *et al.*, 1993; Remy *et al.*, 1994; Jahanshahi *et al.*, 1995; Deiber *et al.*, 1996; Wessel *et al.*, 1997) or microelectrodes in non-human primates (Kurata and Wise, 1988; Mushiake *et al.*, 1991; Romo and Schultz, 1992; Tanji, 1994; Shima *et al.*, 1996; Tanji and Shima, 1996). If the cortical motor areas operate in a network-like fashion, however, they may modulate not only the regional activity of individual areas but also the degree of inter-regional communication ('functional coupling').

Functional coupling of motor areas has not been compared during internally paced and externally paced movements so far. Functional coupling can be assessed by computing correlations between oscillatory activities of different brain regions in the time or frequency domain. In non-human primates, changes in inter-regional cross-correlation measures have been shown to reflect changes in behaviour (Engel *et al.*, 1991*a*, *b*; Murthy and Fetz, 1992; Sanes and Donoghue, 1993; Singer, 1993, 1994; Bressler, 1995; deCharms and Merzenich, 1996; Laurent *et al.*, 1996; Roelfsema *et al.*, 1997). In the frequency domain, coherence analysis has proved to be a useful technique when applied to human EEG data (Rappelsberger and Petsche, 1988; Rappelsberger *et al.*, 1994; Thatcher, 1995; Andrew and Pfurtscheller, 1996; Classen *et al.*, 1998). EEG coherence analysis is complemented by the analysis of regional changes in oscillatory brain activity. In the motor system, this was originally described as 'blocking' of the central μ rhythm (Gastaut *et al.*, 1952; Chatrian *et al.*, 1959), and was later referred to as event-related desynchronization (Pfurtscheller, 1988; Salmelin and Hari, 1994; Toro *et al.*, 1994*a*, *b*; Stancak and Pfurtscheller, 1995, 1996). We now believe it is best to refer to this phenomenon as 'power change' since 'desynchronization' has been used with different meanings with reference to regional spectral power changes and inter-regional coherence, and has thus become ambiguous (Steriade and Amzica, 1996; Steriade *et al.*, 1996*b*).

In the present study, we investigated the functional coupling and regional activation of cortical motor areas during internally paced and externally paced finger movements in healthy volunteers. First, we assessed the regional activation patterns by EEG time domain analysis: we computed movement-related cortical potentials using a new approach that enabled us to study fast repetitive movements (rate, 2/s) with and without metronome pacing (Gerloff *et al.*, 1997). Secondly, we used an approach similar to event-related desynchronization to determine the regional patterns of oscillatory activity. Our approach was based on the spectral power analysis of EEG signals during steady-state task performance. Since the resulting activation patterns were related to task performance rather than to a single event, we refer to this data as task-related power. Finally, we used EEG coherence analysis or task-related coherence to study the functional coupling between the lateral premotor and primary sensorimotor and mesial premotor areas (e.g. SMA), which were, based on the studies mentioned earlier, the areas of our *a priori* interest.

Methods

Subjects

We studied 10 normal volunteers (six men and four women) whose mean age was 34.3 ± 14.0 (SD) years. Nine subjects were right-handed, according to the Edinburgh inventory (Oldfield, 1971), and one was ambidextrous. The data of two subjects had to be excluded because of artefacts (eye blinks, muscle artefacts) and drowsiness towards the end of the session. All subjects included in the final analysis were right-handed (four men, four women; age 32.0 ± 13.3 years). The protocol was approved by the National Institute of Neurological Disorders and Stroke Review Board, and all subjects gave their written informed consent for the study.

Experimental design

Subjects were seated comfortably in an armchair with the right arm relaxed and resting on a pillow. The right hand was positioned palm down at the edge of the pillow so that the fingers could be moved freely. The moving hand was concealed under a small adjustable table.

Subjects performed repetitive, brisk simultaneous extensions of fingers II–V of the right hand followed by brief relaxation (rather than voluntary flexion). Two extensions per second were performed to the beat of a metronome (2 Hz). To avoid intra-session learning effects, subjects practised the required movement before the EEG recording, using on-line EMG feedback.

Four task conditions were studied: externally paced finger extensions, internally paced finger extensions, listening to the metronome without moving, and neither metronome sound nor movement. Each experimental block of trials started with a period of neither metronome sound nor movement, followed by listening to the metronome without moving, externally paced finger extensions and internally paced finger extensions, and ended with a second period of neither metronome sound nor movement. The two periods of neither metronome sound nor movement were used to enable us to check for within-block changes in the background EEG. Since there were no systematic or focal differences between the first and second periods of neither metronome sound nor movement, data from both of these periods were pooled for the final analysis. Three to five (median, four) blocks of 180 movements (corresponding to 90 s) and control conditions (also 90 s) were recorded, alternating with breaks of 1–5 min between blocks to avoid muscular fatigue. During all conditions, subjects looked at a stationary fixation point to prevent eye movement, and were instructed to avoid eye-blinks, swallowing or any movement other than the required finger movements.

Data acquisition

Continuous EEG was recorded from 28 (tin) surface electrodes (Fig. 1), mounted in a cap (Electro-Cap International, Inc., Eaton, Ohio, USA). Impedance was kept below 8 kΩ. Data were sampled at 250 Hz, the upper cutoff was 50 Hz and the time constant was set to DC (DC amplifiers and software by NeuroScan Inc., Herndon, Va., USA). Linked earlobe electrodes served as reference. Four bipolar EMG channels were recorded from surface electrodes positioned over the right and left forearm extensors (extensor digitorum communis, extensor carpi radialis), each pair of electrodes being located ~15 cm apart (distal tendon reference). The high-pass filter for EMG was set to 30 Hz. The EMG was also recorded from corresponding positions on the left forearm to control for mirror movements. Each metronome beat (1 kHz, 130 dB at speaker level, 33.33 ms duration) was automatically documented with a marker in the continuous EEG file.

Data analysis

In order to determine if the motor output was similar in the two movement conditions (externally paced finger extensions and internally paced finger extensions), we analysed the raw and time-averaged EMG. The raw EMG data were inspected visually, and for each subject and movement condition a sample of 100 EMG burst onsets was marked in artefact-free parts of the data file using a computer cursor. The inter-EMG onset intervals were calculated to determine movement rates. In the time-averaged EMG, peak amplitudes and latencies were measured.

The EEG data were analysed using three approaches: (i) movement-related cortical potentials, (ii) task-related power and (iii) task-related coherence.

Movement-related cortical potentials

Artefact rejection and EMG-locked averaging was done off-line. For each subject, a minimum of 180 artefact-free trials was required for each condition (median, 292). The single sweeps were averaged according to the following procedure. After rectification of EMG channels, each EMG onset was marked automatically using a threshold detection algorithm. The averaging time window covered 300 ms before and 200 ms after EMG onset. Linear trend was removed from the EEG channels (linear detrend option of NeuroScan software), and a baseline correction over the entire epoch of 500 ms was computed. Subsequent artefact rejection included three steps: (i) an amplitude threshold rejection criterion was applied to the pre-EMG onset period (only EMG channels) to eliminate all sweeps with EMG background activity before the actual EMG burst; (ii) another threshold rejection algorithm was applied to the EEG channels (entire sweep length) to eliminate all trials contaminated by eye or head movements or electrode artefacts; and (iii) the remaining sweeps were inspected visually to control for minor artefacts that might have escaped the thresholds used. This method has been fully described in an earlier article (Gerloff *et al.*, 1997), particularly with respect to the validation of automatic EMG onset detection and the lack of influence of the tone-evoked response on the movement-related cortical potentials (MRCPs). Peaks were selected by visual inspection of the individual average waveforms and marked with a cursor. Latencies were measured relative to EMG onset. MRCP amplitudes were measured relative to the baseline (base-to-peak). The topographic distribution of the MRCPs was evaluated using amplitude maps (linear four-nearest neighbours interpolation; NeuroScan software) computed on minimum–maximum normalized data (McCarthy and Wood, 1985).

Task-related power

For analysis of task-related power, EEG signals were digitally filtered off-line (1–50 Hz, slope 24 dB/octave) and, for each experimental condition separately, segmented into non-overlapping epochs (disjoint sections; cf. Amjad *et al.*, 1997) of 2048 ms (allowing a frequency resolution of 0.5 Hz). After removal of slow drifts by linear trend correction (linear detrend module of the NeuroScan software) and baseline correction (using the entire window from 0 to 2048 ms), the

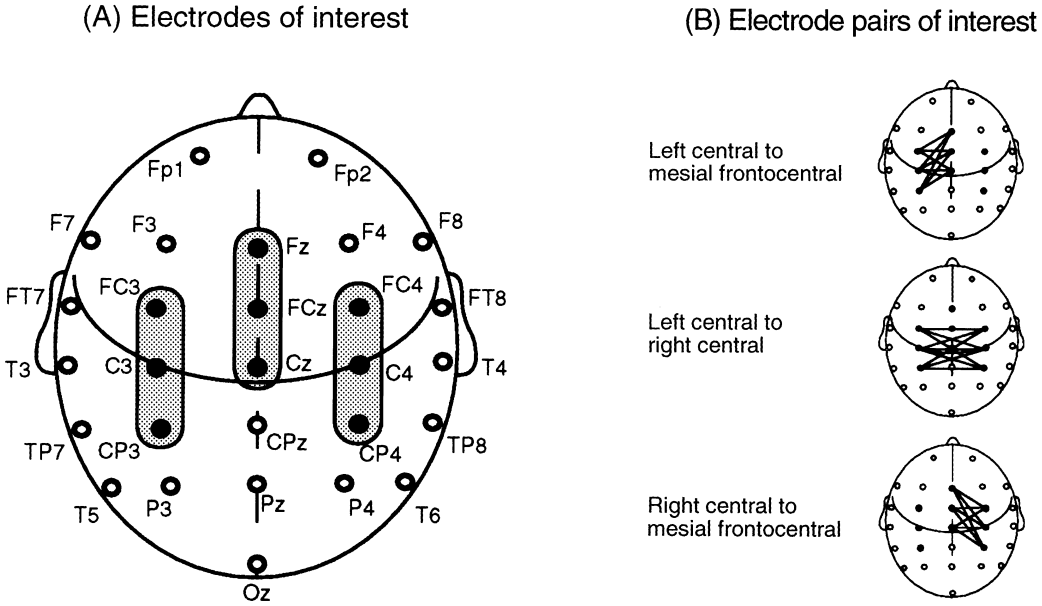

Fig. 1 Electrode montage and electrodes of interest. (**A**) Electrode placement according to the international 10/20 system with additional coronal rows in the central region. The filled circles indicate the nine electrodes of interest that were used for statistical analysis of the task-related power data. The nine electrodes were divided into three groups of three electrodes, each group representing a cortical region: left central, mesial frontocentral, right central (shaded areas). (**B**) Electrode pairs of interest. The three schematic top views of the head show the three major inter-regional links on which the statistical task-related coherence analyses were based. Each major inter-regional link comprises nine individual electrode pairs.

single sweeps were inspected visually, and trials with artefacts were rejected. A minimum of 25 artefact-free trials was required for each condition (median, 54). Each single sweep was Hamming-windowed to control spectral leakage. For spectral power analysis, a discrete Fourier transform was computed for each 2048 ms epoch and all electrodes. Spectral power was calculated for all frequency bins between 1 and 50 Hz (0.5 Hz bin width). In order to reduce the effects of inter-subject and inter-electrode variation in absolute spectral power values, task-related relative power at an electrode *x* ($TRPow_x$) was obtained by subtracting rest ($Pow_{x\ rest}$) from corresponding activation conditions ($Pow_{x\ activation}$), according to equation (1).

$$TRPow_x = Pow_{x\ activation} - Pow_{x\ rest} \quad (1)$$

Therefore, task-related power decreases ('activation') are expressed as negative values while task-related power increases are expressed as positive values. Broad-band power changes were obtained by averaging the power values of the respective frequency bins. This was done for one α (9–11 Hz) and one β (20–22 Hz) frequency range (for selection of frequency ranges and pooling of frequency bins see below).

Task-related coherence

Coherence is computed in the frequency domain and is a normalized measure of the coupling between two signals at any given frequency (Schoppenhorst *et al.*, 1980; Shaw, 1984; Rappelsberger and Petsche, 1988; Farmer *et al.*, 1993; Conway *et al.*, 1995; Weiss *et al.*, 1996; Salenius *et al.*, 1997; Classen *et al.*, 1998). For task-related coherence analysis, EEG signals were filtered, segmented, corrected for trend and baseline, inspected for artefacts, Hamming-windowed and Fourier-transformed as described for task-related power. A minimum of 25 artefact-free trials was required for each condition (median, 54 disjoint sections). The coherence values were calculated for each frequency bin λ according to equation (2) (implemented in commercial software by NeuroScan).

$$Coh_{xy}(\lambda) = |R_{xy}(\lambda)|^2 = \frac{|f_{xy}(\lambda)|^2}{f_{xx}(\lambda)\, f_{yy}(\lambda)} \quad (2)$$

Equation (2) is the extension of the Pearson's correlation coefficient to complex number pairs. In this equation, *f* denotes the spectral estimate of two EEG signals *x* and *y* for a given frequency bin (λ). The numerator contains the cross-spectrum for *x* and *y*(f_{xy}), the denominator the respective autospectra for *x*(f_{xx}) and *y*(f_{yy}). For each frequency λ, the coherence value (Coh_{xy}) is obtained by squaring the magnitude of the complex correlation coefficient *R*, and is a real number between 0 and 1. In association with coherence, phase information is also available, but was not included in the present analysis. In order to reduce the effect of inter-subject and inter-electrode pair variation in absolute coherence values, task-related relative coherence ($TRCoh_{xy}$) was obtained by subtracting rest ($Coh_{xy\ rest}$) from

corresponding activation conditions ($Coh_{xy\ activation}$), according to equation (3).

$$TRCoh_{xy} = Coh_{xy\ activation} - Coh_{xy\ rest} \quad (3)$$

Therefore, coherence magnitude increments are expressed as positive values and coherence decrements are expressed as negative values. Coherence increments or decrements between baseline and movement conditions for each pair of electrodes were displayed as colour-coded 'link' plots, which permitted the inspection of the magnitude and spatial patterns of task-related coherence. This method also eliminates the bias in the absolute coherence introduced by the reference electrodes (Fein *et al.*, 1988; Rappelsberger and Petsche, 1988; Classen *et al.*, 1998). To obtain broad-band coherence values, $Coh_{xy}(\bar{\lambda})$, $Coh_{xy}(\lambda_j)$ was averaged over frequency bins $j = \lambda_{min}$ to λ_{max} (λ_{min} and λ_{max} corresponding to the lower and upper frequency bins in the chosen frequency band). To average the frequency bins we used the concept of pooled coherence as described by Amjad *et al*. (1997). The number of frequency bins pooled was equal for all subjects, electrode pairs and conditions. Broad-band coherence was calculated for two different frequency bands: α (9–11 Hz) and β (20–22 Hz). These frequencies were selected for several reasons. First, they have previously been shown to be particularly sensitive to movement-related changes in cortical oscillatory activity in humans (Tiihonen *et al.*, 1989; Salmelin and Hari, 1994). Secondly, on visual inspection of the original task-related coherence spectra they represented the frequency ranges within which the two conditions differed most consistently (Fig. 4). Thirdly, they had sufficient spectral power in all individuals studied.

Statistical analysis

The non-parametric Wilcoxon matched pairs test was employed to compare amplitudes and latencies of the time-averaged rectified EMG and the inter-EMG onset intervals between the externally paced and internally paced finger extensions conditions.

The Wilcoxon matched pairs test was also used to compare the amplitudes of the early premovement component and of the previously described lateralized parietal–negative premovement and frontal–negative post-movement MRCP components between externally paced finger extensions and internally paced finger extensions. Differences were considered significant if $P < 0.05$.

Subtraction of power and coherence values as shown in equations (1) and (3) may be used to demonstrate mean task-related changes of the mean values (Figs 5 and 6). However, power and coherence values have certain properties which make it necessary to transform them prior to further statistical evaluation (Rosenberg *et al.*, 1989; Farmer *et al.*, 1993; Halliday *et al.*, 1995; Amjad *et al.*, 1997). For spectral power values, which are real numbers $\geqslant 0$, the variance decreases when the mean approaches zero. For coherence values, which are real numbers between 0 and 1, the variance decreases for values at both ends of the range. The transformations described below were therefore applied in order to stabilize the variances for both task-related power and task-related coherence values.

The variance of spectral power estimates can be stabilized by logarithmic (log) transformation (Halliday *et al.*, 1995). In the present data this procedure was observed to give approximately constant residual variance across all levels of the response. Thus, for the statistical analysis, equation (1) becomes equation (4).

$$logTRPow_x = log[Pow_{x\ activation}] - log[Pow_{x\ rest} \quad (4)$$

For coherence estimates, the hyperbolic inverse tangent ($tanh^{-1}$) transformation normalizes the underlying distribution of correlation coefficients and stabilizes the variances of the distributions (Rosenberg *et al.*, 1989; Farmer *et al.*, 1993). The $tanh^{-1}$ transformation was applied to each individual data set prior to subtraction of the coherence estimates in order to compute the task-related coherence task-related coherence. Thus, for the statistical analysis equation (3) becomes equation (5).

$$tanh^{-1}TRCoh_{xy} = tanh^{-1}[Coh_{xy\ activation}] - tanh^{-1}[Coh_{xy\ rest} \quad (5)$$

The logTRPow and $tanh^{-1}$, task-related coherence values were computed for the internally paced and externally paced finger extensions conditions and were entered into separate factorial analyses of variance (ANOVAs). For logTRPow, factors were condition (externally paced finger extensions, internally paced finger extensions) and region. For $tanh^{-1}$ task-related coherence, factors were condition (externally paced finger extensions, internally paced finger extensions) and connection. The definition of regions and connections is described below in detail and illustrated in Fig. 1. Differences in the absolute coherence levels between subjects and between electrodes were minimized by the subtractive approach, because only differences between active and rest conditions were considered. The α (9–11 Hz) and β (20–22 Hz) bands were analysed separately.

We defined electrodes of interest (EOI) and electrode pairs of interest (POI), which is similar to the region-of-interest (ROI) approach that has been used in neuroimaging techniques such as PET, magnetic resonance spectroscopy and single-photon emission tomography (Rascol *et al.*, 1993, 1994; Shibasaki *et al.*, 1993). EOI and POI were chosen on the basis of prior anatomical and physiological knowledge. We included electrodes known to overlie approximately the lateral premotor cortex and SM1 of the left and right hemispheres (left, FC3, C3, CP3; right, FC4, C4, CP4) and the mesial frontocentral cortex including the SMA (Fz, FCz, Cz) (Homan *et al.*, 1987; Steinmetz *et al.*, 1989; Gerloff *et al.*, 1996). To pool the coherence estimates across electrode pairs we used the method described by Amjad *et al*. (1997). Weighting of the pooled coherences was not necessary because the number of electrode pairs was equal for all connections, conditions and subjects.

For logTRPow analysis, the nine EOI were grouped into

three regions each represented by three electrodes: 'left central' (FC3, C3, CP3), 'right central' (FC4, C4, CP4) and 'mesial frontocentral' (Fz, FCz, Cz) (Fig. 1, left). The factor Region was integrated into the ANOVA to test differences between activation of contralateral and ipsilateral lateral premotor cortex and SM1 and mesial premotor areas.

For $\tanh^{-1}$ task-related coherence analysis, the total number of links between the EOI was 27 (27 POI), and these were grouped into three major connections: 'left central to right central' (FC3–FC4, FC3–C4, FC3–CP4, C3–FC4, C3–C4, C3–CP4, CP3–FC4, CP3–C4, CP3–CP4), 'left central to mesial frontocentral' (FC3–Fz, FC3–FCz, FC3–Cz, C3–Fz, C3–FCz, C3–Cz, CP3–Fz, CP3–FCz, CP3–Cz) and 'right central to mesial frontocentral' (FC4–Fz, FC4–FCz, FC4–Cz, C4–Fz, C4–FCz, C4–Cz, CP4–Fz, CP4–FCz, CP4–Cz) (Fig. 1, right). The factor Connection was integrated into the ANOVA to test differences between the different functional links of contralateral and ipsilateral lateral premotor cortex and SM1 and mesial premotor areas. In addition, to test whether the $\tanh^{-1}$ task-related coherence effects observed in the preselected POI were topographically restricted (as opposed to global in all electrode pairs), we applied the same statistical procedure to 27 randomly chosen pairs of electrodes (excluding the POI): FC3–OZ, CP3–FP2, F3–OZ, TP7–PZ, F7–CPZ, T5–OZ, FP1–F7, FT7–TP7, F3–FT7, FZ–F8, P4–FT8, TP8–FP2, T6–CPZ, FP2–PZ, OZ–TP8, FCZ–TP8, F8–T6, F8–PZ, P3–F4, TP7–FT8, TP7–T6, F3–FT8, P3–FT8, FP1–T6, T5–FT8, T5–F8 and F7–T4.

Further, to determine how the 27 POI were exceptional among all possible random combinations of 27 electrode pairs (i.e. topographical specificity), we examined the sampling distribution of the mean of 27 randomly chosen pairs of electrodes from the total population of 378 pairs. The central limit theorem states that the sampling distribution reasonably approximates a Gaussian distribution. Hence, we calculated the *Z* scores of the mean of 27 POI in each condition according to equation (6).

$$Z = \frac{\overline{\tanh^{-1}\mathrm{TRCoh}_{\mathrm{POI}}} - \overline{\tanh^{-1}\mathrm{TRCoh}_{\mathrm{TOTAL}}}}{\mathrm{SEM}_{27}} \qquad (6)$$

where $\overline{\tanh^{-1}\mathrm{TRCoh}_{\mathrm{POI}}}$ is the mean task-related coherence for the 27 POI, $\overline{\tanh^{-1}\mathrm{TRCoh}_{\mathrm{TOTAL}}}$ is the mean task-related coherence of all 378 electrode pairs and SEM_{27} is the standard error of the mean for samples of the size of 27. In this situation, $Z = 1.65$ corresponds to $P = 0.05$, P denoting the probability of finding one or more combinations of 27 electrode pairs with a mean task-related coherence higher than $\overline{\tanh^{-1}\mathrm{TRCoh}_{\mathrm{POI}}}$. We calculated the *Z* scores for the 27 randomly chosen pairs of electrodes accordingly, in order to characterize their position in the population distribution (i.e. to decide whether they constituted a representative control sample).

Significance levels obtained from multiple tests on the same data pool were Bonferroni-corrected.

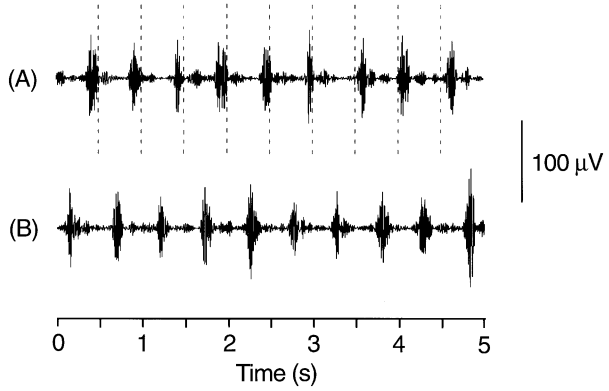

Fig. 2 EMG, extensor digitorum muscle of the right forearm. Raw data are given for an individual subject. There was no systematic difference between EMG patterns associated with externally paced finger extensions (**A**) and internally paced finger extensions (**B**). After a practice session, all subjects could maintain a stable movement rate of ~2 Hz in both movement conditions. The dashed vertical lines indicate the metronome sounds.

Results

The movements were similar in the two conditions (Fig. 2). Peak latencies were not significantly different (externally paced finger extensions, 37 ± 12 ms; internally paced finger extensions, 38 ± 10 ms) and amplitudes (externally paced finger extensions, 45 ± 28 μV; internally paced finger extensions, 44 ± 23 μV) of the time-averaged EMG bursts and mean movement rates (externally paced finger extensions, 1.9 ± 0.0 Hz; internally paced finger extensions, 1.9 ± 0.1 Hz) were not significantly different.

Movement-related cortical potentials

Figure 3 shows an overlay of the grand average MRCP waveform associated with internally and externally paced finger extensions at electrode FCz, and a topographic map of the difference waveforms (internally paced finger extensions minus externally paced finger extensions). Main MRCP components were a premovement peak and a post-movement peak, as previously described with this paradigm (Gerloff *et al.*, 1997). In addition, an early negativity was observed that occurred only with internally paced movements. This early negativity, associated with internally paced finger extensions, was prominent in frontocentral midline electrodes (particularly in electrode FCz), and extended into electrodes F3, FC3 and C3. The amplitude difference between externally paced finger extensions (0.3 ± 0.6 μV) and internally paced finger extensions (–0.9 ± 0.8 μV), measured in electrode FCz at a latency of 168 ± 49 ms before EMG onset, was significant ($P < 0.05$, Wilcoxon matched pairs test).

Latencies and amplitudes of the premovement peak, measured in electrode P3, were –57 ± 49 ms and –1.4 ± 0.8 μV for externally paced finger extensions, and –49 ± 65 ms and –1.2 ± 0.7 μV for internally paced finger extensions. Latencies and amplitudes of the post-movement peak, measured in electrode F3, were 104 ± 24 ms and –1.4 ± 0.2

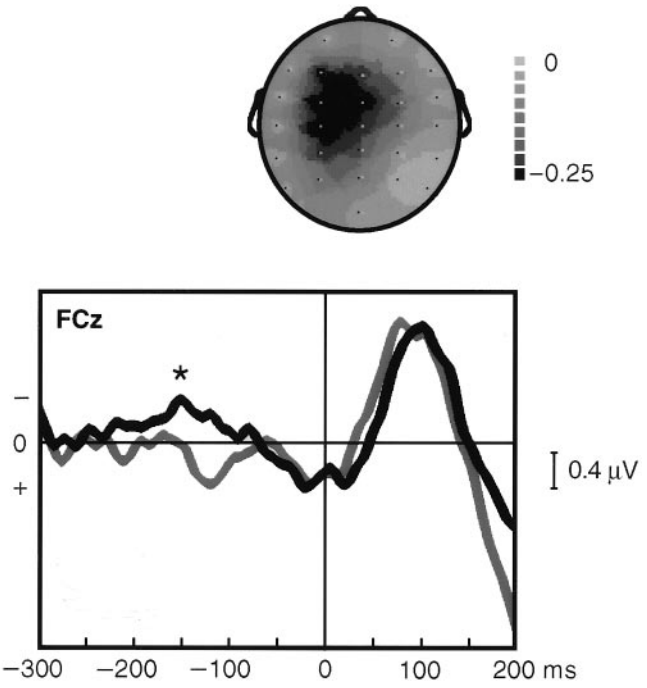

Fig. 3 Movement-related cortical potentials (steady-state MRCPs). *Top*: difference map (internally paced minus externally paced finger extensions at 170 ms before EMG onset). Negative values (grey to black) indicate greater negative movement-related cortical potential amplitudes during internally compared with externally paced finger extensions. The area of increased negativity during internally paced finger extensions included the frontocentral midline electrodes (e.g. FCz) and extended towards electrodes F3, FC3 and C3 over the left hemisphere. *Bottom*: grand average ($n = 8$) waveforms at electrode FCz. Overlay of movement-related cortical potentials associated with externally paced (grey) and internally paced (black) finger extension movements. The vertical line indicates EMG onset (0 ms). Note the amplitude difference between conditions occurring ~170 ms before EMG onset (*). At this latency in electrode FCz, only internally paced movements were associated with a negative deflection ($P < 0.05$, Wilcoxon matched pairs test), which could be consistent with additional premovement activation of the mesial frontocentral cortex, including the region of the SMA.

μV for externally paced finger extensions, and 96 ± 22 ms and –1.2 ± 0.5 μV for internally paced finger extensions. No significant differences between conditions were observed for these peaks (Wilcoxon matched pairs test). For both the externally and the internally paced finger extension condition, the topographical distribution of the premovement peak and post-movement peak corresponded well with the topography originally described with this paradigm, with a parietal-negative electrical field immediately before EMG onset (premovement peak) and a frontal-negative, parietal-positive field after EMG onset (post-movement peak) (Gerloff *et al.*, 1997).

In summary, MRCP analysis suggested an early (~170 ms before EMG onset), relatively low-voltage but yet significant additional negative deflection, particularly over the mesial and left frontocentral cortex, in association with internally paced movements.

Task-related power

As noted earlier, the frequency bands of interest were determined on the basis of visual inspection of the coherence spectra (averaged across subjects), because task-related coherence was the primary target of the study. Figure 4 shows the spectra in 1 Hz steps for the externally paced and internally paced finger extension conditions.

Figure 5 shows the topographic task-related power maps. The largest task-related power decreases ('activation') for both movement conditions occurred in the α band over the left central region (electrodes FC3, C3 and CP3). In the β band, the maximal task-related power decrease was even more confined to electrode C3. The main difference between the externally paced and internally paced finger extension conditions was spatial extension of the task-related power decrease towards Fz, FCz and, to a smaller extent, Cz in the α band (Fig. 5). Increases in spectral power occurred in the α band over the occipital and parieto-occipital cortex, which probably reflects the fact that our subjects were not allowed to use visual feedback for controlling the movements, putting the occipital cortex in an idling state (Pfurtscheller, 1992).

The statistical results for task-related power are summarized in Table 1. As for the task-related power in the nine EOI (FC3, C3, CP3, Fz, FCz, Cz, FC4, C4 and CP4), the major difference in spectral power between conditions occurred in the α band (9–11 Hz) ($P = 0.0047$; ANOVA, main effect for Condition; internally paced, –0.129 ± 0.018 μV^2 externally paced, –0.065 ± 0.017 μV^2, log-transformed mean ± 1 SE). No differences were observed in the β band. This is reflected in the topographic maps (Fig. 5). In both movement conditions, the maximum of the α task-related power decrease occurred in the electrode group overlying the left central region (FC3, C3 and CP3) ($P = 0.0001$; ANOVA, main effect for Region), with larger task-related power decreases during the internally paced than during the externally paced finger extension condition. The α task-related power decrease over the midline (Fz, Fcz and Cz) and right central (FC4, C4 and CP4) electrodes was also larger during internally paced than during externally paced finger extensions. There was no significant interaction of Condition with Region in the α band, indicating that the task-related power amplitude differences between the three regions were not significantly different for internally paced and externally paced movements.

In the β band, the ANOVA main effect for Region was also significant ($P = 0.0027$), indicating topographic differentiation in this band as well. This was mostly related to larger task-related power decreases over the left central and mesial frontocentral region (Fig. 5) compared with the right central electrode group, particularly in the externally paced finger extension condition. The log-transformed task-related power mean values are displayed in Fig. 7.

In summary, the task-related power results suggest that in the α frequency range (9–11 Hz), internally paced movements are associated with higher regional activation of the bilateral

premotor and sensorimotor cortex and of the mesial frontocentral premotor cortex than are externally paced movements. According to the topographic maps (Fig. 5), the most prominent feature of the α task-related power decrease is the extension of the activated area over the mesial frontocentral cortex, including the region of the SMA during internally paced movements.

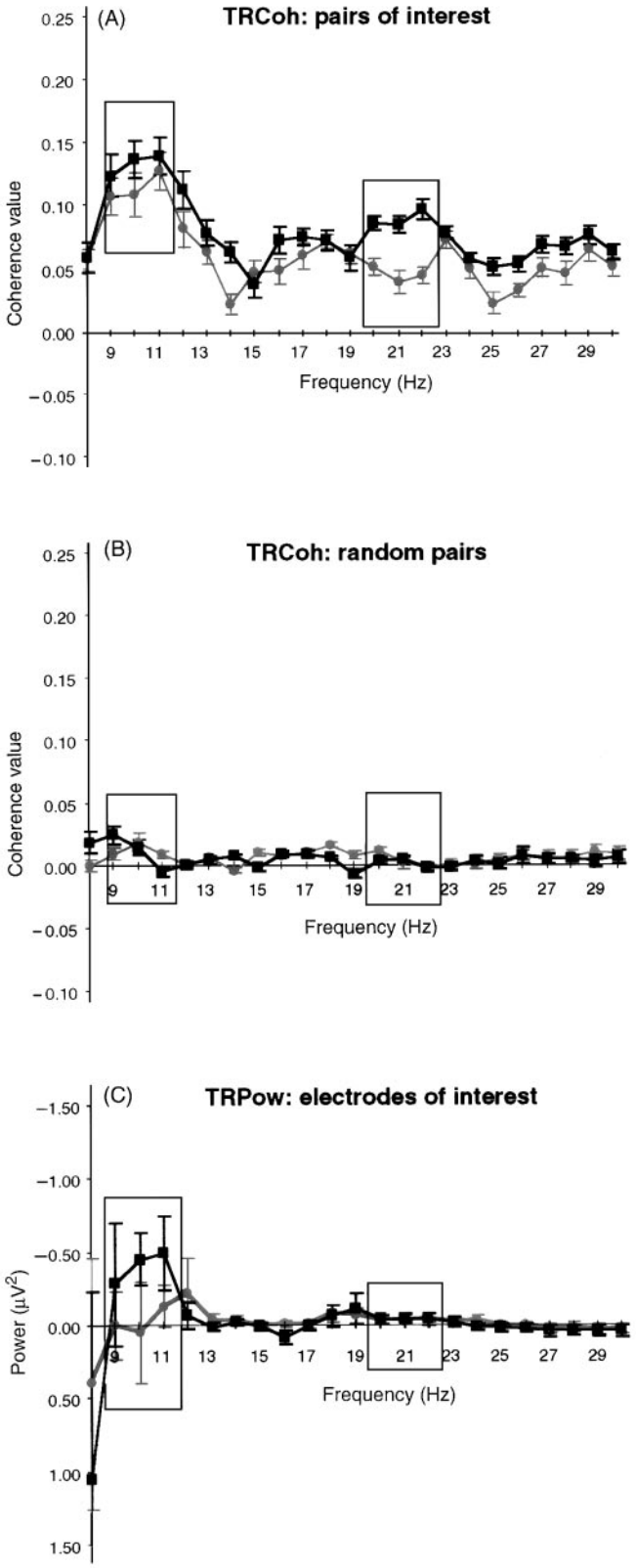

Task-related coherence

Figure 4 shows the task-related coherence spectra in 1 Hz steps for the relevant frequency range, plotted as overlays for the externally paced and internally paced finger extension conditions, and separately for the 27 POI and the 27 randomly chosen pairs of electrodes. In the POI plot, two frequency bands of prominent differences between internally paced and externally paced finger extensions were detected visually: 9–11 Hz in the α band and 20–22 Hz in the β band. The analysis of the task-related coherence data was then continued for these two broad bands (task-related power analysis was done in the identical frequency bands). The corresponding plot of the coherence spectrum for the randomly chosen pairs of electrodes showed no systematic differences between the internally paced and externally paced finger extension conditions, indicating that the changes observed in the POI were not globally present in any given electrode pair. The conclusion that the task-related coherence changes were not global but, instead, spatially restricted was further supported by the *Z*-score analysis. The *Z* scores for the POI during performance of externally and internally paced movements were greater than 1.65 (corresponding to $P < 0.05$) for both the α and β frequency bands. None of the *Z* scores that were computed accordingly for the randomly chosen pairs of electrodes exceeded ±1.65. This supported our *a priori* hypothesis that the POI selected were relevant for the tasks chosen. The *Z*-score results also suggested that the randomly chosen pairs of electrodes which we selected for further statistical analysis were representative of the distribution.

Figure 6 shows the topographic task-related coherence maps for both movement conditions and the two frequency bands. The statistical results are summarized in Table 2. In general, increases in task-related coherence were the most prominent task-related change, and these were typically

Fig. 4 Group data for coherence and power spectra during internally (black) and externally (grey) paced movements ($n = 8$). Error bars indicate 2 SEM. Each data point represents an average of two 0.5 Hz bins of the fast Fourier spectrum, and of 27 electrode pairs (**A** and **B**) or nine electrodes (**C**), respectively, in eight subjects. Windows indicate the frequency ranges in which the differences between the two movement conditions were most prominent (9–11 Hz, 20–22 Hz), and that were therefore used for task-related coherence (TRCoh) and task-related power (TRPow) computations. (**A**) Task-related coherence, 27 electrode pairs of interest; (**B**) task-related coherence, 27 randomly chosen electrode pairs. Note the lack of significant task-related coherence values in either movement condition, indicating that the task-related coherence changes seen in the top panel (pairs of interest) were not global. (**C**) Task-related power, nine electrodes of interest. Note the clear difference between the movement conditions in the α range, but the lack of similar differences in higher frequency ranges.

restricted to the central region, the highest number of functional links converging on electrodes C3, CP3 and CP4 in all frequency bands. Task-related coherence decreases occurred in the frontal and temporal regions, particularly in the β band. On visual inspection, the major difference between externally paced and internally paced finger extensions was an increased density of functional links between lateral and mesial central regions bilaterally with internally paced

Table 1 *Statistical analysis (ANOVA): task-related power, log-transformed data*

	Test	*F*	*P*
α band			
All EOI	Main effect for Condition	8.2	0.0047*
	Main effect for Region	13.0	0.0001*
	Interaction Condition × Region	0.0	0.9567
Left central	Contrast analysis$_{CONDITION}$	2.2	0.1593
Mesial frontocentral	Contrast analysis$_{CONDITION}$	3.2	0.0767
Right central	Contrast analysis$_{CONDITION}$	3.2	0.0781
β band			
All EOI	Main effect for Condition	0.5	0.5053
	Main effect for Region	6.2	0.0027*
	Interaction Condition × Region	0.0	0.9782
Left central	Contrast analysis$_{CONDITION}$	0.2	0.6806
Mesial frontocentral	Contrast analysis$_{CONDITION}$	0.1	0.8219
Right central	Contrast analysis$_{CONDITION}$	0.3	0.6047

*Significant after Bonferroni correction.

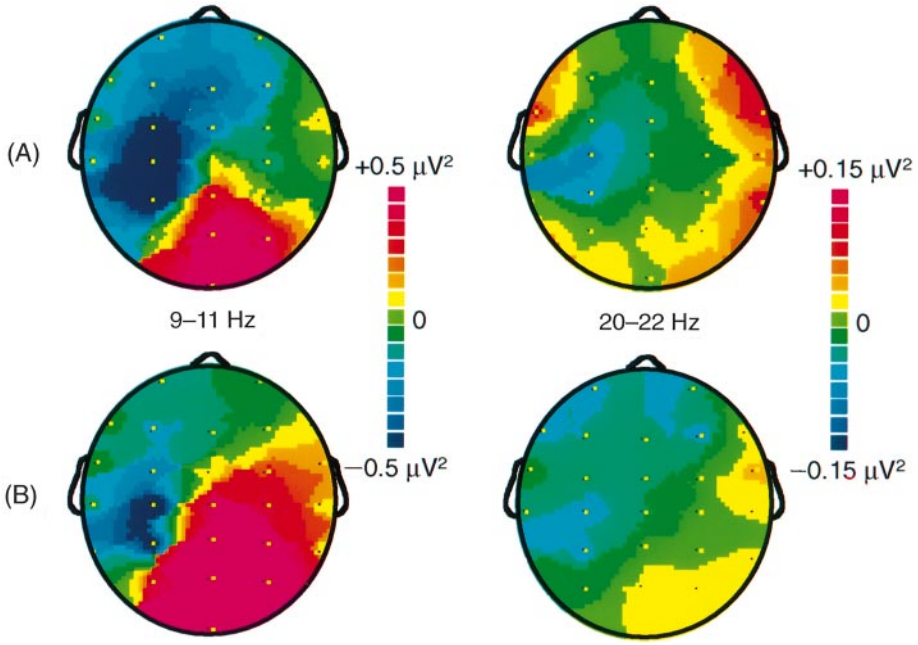

Fig. 5 Grand average of topographic task-related power maps (n = 8). The dots indicate electrode positions. Task-related power decreases (areas of 'activation', negative task-related power values) are coded in blue and power increases (positive task-related power values) are coded in red/pink. The maximum of task-related power decreases for both movement conditions was located over left central electrodes, particularly over C3, with higher amplitudes in the 9–11 Hz band than in the 20–22 Hz band. During internally paced finger movements (**A**), in the 9–11 Hz band the area of task-related power decrease extended from left central electrodes FC3, C3 and CP3 towards the frontocentral midline including electrodes FCz and Fz, as well as F3, suggesting additional activation of the mesial frontocentral cortex, including the region of the SMA. In the 9–11 Hz band, pronounced task-related power increases occurred over the occipital and parieto-occipital regions, possibly reflecting an 'idling state' of these regions, since visual feedback was prevented. In the 20–22 Hz band, with internally paced finger extensions there was a slightly greater task-related power decrease in electrode C3 compared with externally paced finger extensions (**B**), but the difference was not significant. The scales were adjusted to the overall amplitudes of task-related power in each frequency band to facilitate comparison between the two movement conditions.

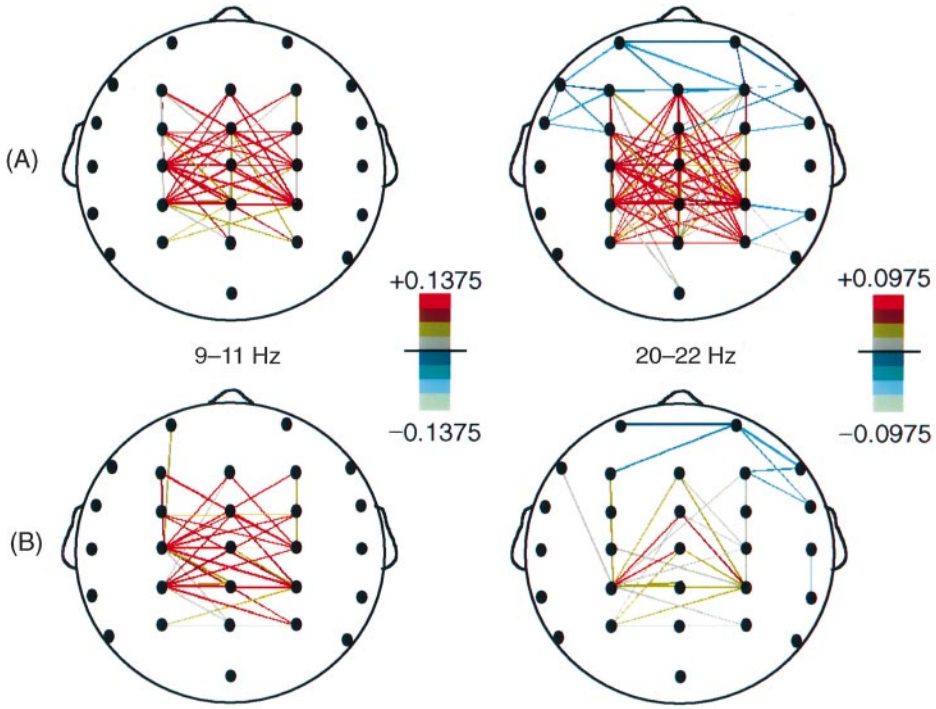

Fig. 6 Grand average of topographic task-related coherence maps ($n = 8$). The dots indicate electrode positions. Task-related coherence changes are shown in colour-coded lines. Red lines indicate maximal task-related coherence increases ('functional coupling') and light green indicates maximal task-related coherence decreases ('decoupling'). In order to allow the identification of the most prominent links, only task-related coherence values exceeding a threshold of ±0.10 (9–11 Hz) or ±0.06 (20–22 Hz) are displayed. The scales are adjusted to the overall amplitudes of task-related coherence in each frequency band to facilitate comparison between the two movement conditions. In all frequency bands and both types of movements [internally paced finger extensions (**A**); externally paced finger extensions (**B**)], task-related coherence increases were focused over the central region with a maximum of links converging on electrode C3, and to a smaller extent CP3 and CP4. With both internally paced and externally paced finger extensions, links were present between left and right lateral central electrodes and between left central and mesial frontocentral electrodes. The main difference between conditions was the increased amplitude and number of links between bilateral and mesial premotor and sensorimotor areas during internally paced finger extensions. This was most prominent in the 20–22 Hz band ($P = 0.0001$, ANOVA). In the 9–11 Hz frequency range, this difference between conditions was smaller but not significant ($P = 0.0841$, ANOVA). Note also the additional links that occurred during internally paced finger extensions between left central, mesial frontocentral and right parietal (P4) regions, particularly in the 20–22 Hz frequency band.

Table 2 Statistical results (ANOVA): task-related coherence, $\tanh^{-1}$-transformed data

	Test	*F*	*P*
α band			
All POI	Main effect for Condition	3.7	0.0549
	Main effect for Connection	1.2	0.3139
	Interaction Condition×Connection	0.2	0.8416
Left central to mesial frontocentral	Contrast analysis$_{CONDITION}$	0.7	0.4119
Left central to right central	Contrast analysis$_{CONDITION}$	0.9	0.3555
Right central to mesial frontocentral	Contrast analysis$_{CONDITION}$	2.5	0.1132
β band			
All POI	Main effect for Condition	32.2	0.0001*
	Main effect for Connection	1.2	0.1091
	Interaction Condition × Connection	0.8	0.4397
Left central to mesial frontocentral	Contrast analysis$_{CONDITION}$	12.4	0.0005*
Left central to right central	Contrast analysis$_{CONDITION}$	16.4	0.0001*
Right central to mesial frontocentral	Contrast analysis$_{CONDITION}$	5.2	0.0234

*Significant after Bonferroni correction.

extensions. In addition, more prominent links occurred between left central, mesial frontocentral and right parietal regions during internally paced than during externally paced finger extensions (electrode P4, particularly in the β band). While the absolute task-related coherence values (all POI pooled) were higher in the α than in the β band, the differences between externally paced and internally paced finger extension conditions were generally more prominent in the β band.

Accordingly, the ANOVA main effect for Condition only approached significance for the α band ($P = 0.0549$), and was highly significant for the β band ($P = 0.0001$). The most significant increases in task-related coherence between externally paced and internally paced finger extensions occurred in the β band between the left and right central regions ($P = 0.0001$) and between the left central and mesial frontocentral regions ($P = 0.0005$). The difference between externally paced and internally paced finger extensions tended to be less pronounced between right central and mesial frontocentral regions ($P = 0.0234$). In the α band, contrast analysis revealed no significant differences between movement conditions for any of the inter-regional links. The task-related coherence mean values are illustrated in Fig. 7.

The main effect Connection was not significant for either of the frequency bands, reflecting the fact that the task-related coherences for the three different inter-regional links (right to left central, left central to mesial frontocentral and right central to mesial frontocentral) were not significantly different from each other. Similarly, the interaction Condition × Connection was not significant, indicating that the task-related coherence differences between internally paced and externally paced finger extensions were not significantly different for the three inter-regional main links.

Following exactly the same statistical procedures for the 27 randomly chosen electrode pairs, no significant ANOVA main effects were observed. In particular, the main effect for Condition was not significant in any of the frequency bands. This indicates that the significant differences in functional coupling between externally paced and internally paced movements, as observed in the POI, were topographically restricted and not a global phenomenon.

Figure 8 illustrates the $\tanh^{-1}$-transformed task-related coherence data for an individual subject. Displayed is one representative electrode pair (CP3–Cz), which is part of the pooled coherence for the connection left central to mesial frontocentral, and another (CP3–CP4) which is part of the connection left to right central. This plot of individual (unpooled) task-related coherence provides an example of a clear difference between internally paced and externally paced finger extensions in the β band (particularly 21 and 22 Hz in this subject) and the absence of a consistent difference between internally paced finger extensions and externally paced finger extensions in the α band. The standard errors displayed in Fig. 8 were computed from the number of disjoint sections for each condition (Rosenberg *et al.*, 1989; Farmer *et al.*, 1993).

In summary, the task-related coherence findings suggest that internal pacing of movement is associated with greater functional coupling of cortical premotor and sensorimotor areas than external pacing, particularly with increased movement-related interhemispheric coupling of the lateral premotor cortex/SM1 regions bilaterally, and with increased coupling of the left lateral premotor cortex/SM1 region (contralateral to the moving hand) and the region of the SMA. These changes were most prominent in the β frequency band (20–22 Hz).

Discussion

Our results show that simple internally paced and externally paced finger movements are associated with different patterns of functional coupling and regional activation of human cortical motor areas. Time domain analysis (MRCPs) pointed to additional involvement of the mesial frontocentral cortex in the premovement period, ~170 ms before EMG onset, with internally paced movements. In agreement with this observation, the analysis of regional oscillatory activity (task-related power) demonstrated that the activated area, which was relatively focused over the contralateral central region during externally paced movements, extended over the mesial frontocentral cortex and towards the premotor and sensorimotor cortex ipsilateral to the moving hand with internally paced movements. In addition, coherence analysis suggested that the functional coupling of premotor and sensorimotor areas was different depending on the mode of pacing, with larger inter-regional coupling during internally paced movements. To some extent these differences between movement conditions were frequency band-specific, with the greatest differences of regional oscillatory activation in the α band (9–11 Hz, task-related power) and the most prominent differences in functional coupling in the β band (20–22 Hz, task-related coherence). This indicates that modulation of oscillatory activity in different frequency ranges may reflect distinct aspects of information processing in a cortical motor network. In general, the particular sensitivity of these two frequency ranges to motor task-related changes corresponds well with previous EEG (Pfurtscheller, 1981; Stancak and Pfurtscheller, 1995) and MEG (magnetoencephalogram) (Tiihonen *et al.*, 1989; Salmelin and Hari, 1994) findings.

Cortical areas involved in generation of internally and externally paced movements

The topographic distributions of MRCP waveforms and task-related power (α and β bands) point to activation of (i) the contralateral sensorimotor (primary motor and primary sensory) cortex, and probably also the lateral premotor cortex (area 6) for both internally paced and externally paced movements, (ii) the mesial frontocentral cortex, including the region of the SMA during internally paced movements,

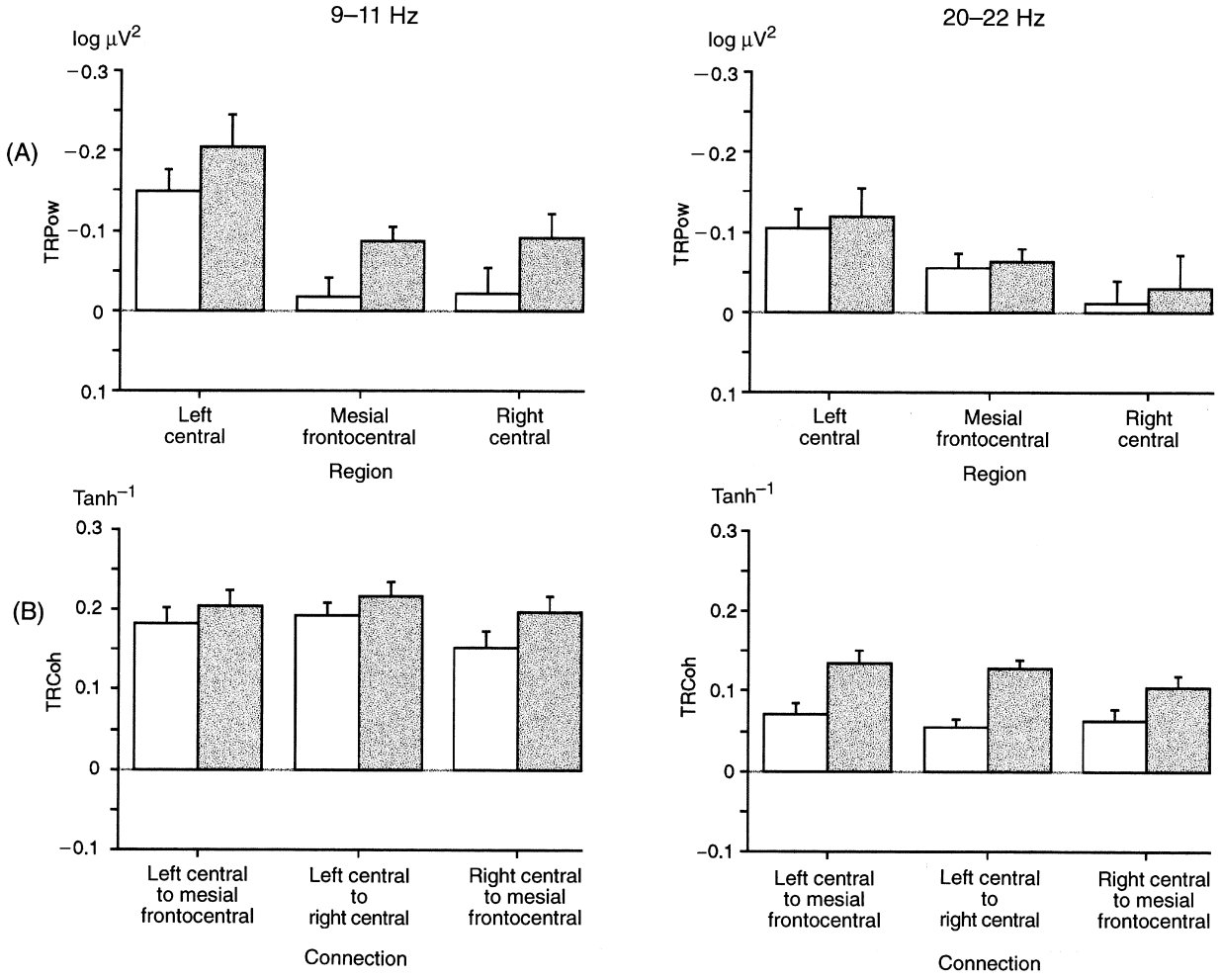

Fig. 7 Means and variances of task-related power (**A**) and task-related coherence (**B**) group values in the regions and connections of interest. Task-related power regions: left central region (overlying the left lateral premotor and primary sensorimotor cortex), frontocentral midline (mesial frontocentral cortex including the region of the SMA), right central region (homologous to left central). Task-related coherence connections: left frontocentral region to frontocentral midline, interhemispheric coupling between left and right lateral premotor and primary sensorimotor region, right frontocentral region to frontocentral midline (analogous to left frontocentral region to frontocentral midline). Open columns = externally paced finger extensions; grey columns = internally paced finger extensions. Error bars: ±1 SE. *Significant differences as revealed by contrast analysis ($P < 0.05$ after Bonferroni correction).

and (iii) the ipsilateral sensorimotor and probably premotor cortex during internally paced movements.

The possible electrical sources of the so-called 'steady-state' MRCPs associated with externally paced movements (i.e. the primary motor and primary sensory cortex) have been discussed in detail elsewhere (Gerloff *et al.*, 1997). The additional negative deflection occurring 170 ms before EMG onset with internally paced movements had its topographic maximum over FCz, extending to F3, FC3 and C3, and would therefore be consistent with additional activation of the mesial frontocentral cortex, probably including the SMA. It is not entirely clear how reliably SMA activity is reflected in scalp-recorded, time-averaged potentials such as MRCPs or the Bereitschaftspotential (Deecke and Kornhuber, 1978; Barrett *et al.*, 1986; Deecke, 1987; Deecke *et al.*, 1987; Lang *et al.*, 1990, 1991; Boetzel *et al.*, 1993; Toro *et al.*, 1993; Gerloff *et al.*, 1996; Hallett and Toro, 1996; Mackinnon *et al.*, 1996; Marsden *et al.*, 1996). However, there is evidence from EEG source modelling experiments (Toro *et al.*, 1993; Knosche *et al.*, 1996), in patients with SMA lesions (Deecke *et al.*, 1987; Lang *et al.*, 1991), patients with Parkinson's disease (Dick *et al.*, 1987, 1989; Cunnington *et al.*, 1995; Praamstra *et al.*, 1996), from subdural recordings (Ikeda *et al.*, 1992, 1993, 1996) and from correlative EEG and PET studies (Jahanshahi *et al.*, 1995; Mackinnon *et al.*, 1996) that SMA activation relates to some extent to MRCP amplitude changes with topographic maximum in the frontocentral midline electrodes (Fcz and Cz) (Marsden *et al.*, 1996).

In the present study, the concept of additional activation of the mesial frontocentral cortex during internally paced movements was further supported by the results of EEG frequency domain analysis. Regional power decreases are thought to reflect increased activity of extended neuronal assemblies in the underlying cortex (Jasper and Penfield, 1949; Lopes da Silva *et al.*, 1980; Papakostopoulos *et al.*, 1980; Pfurtscheller, 1988; Toro *et al.*, 1994*a*, *b*; Stancak and

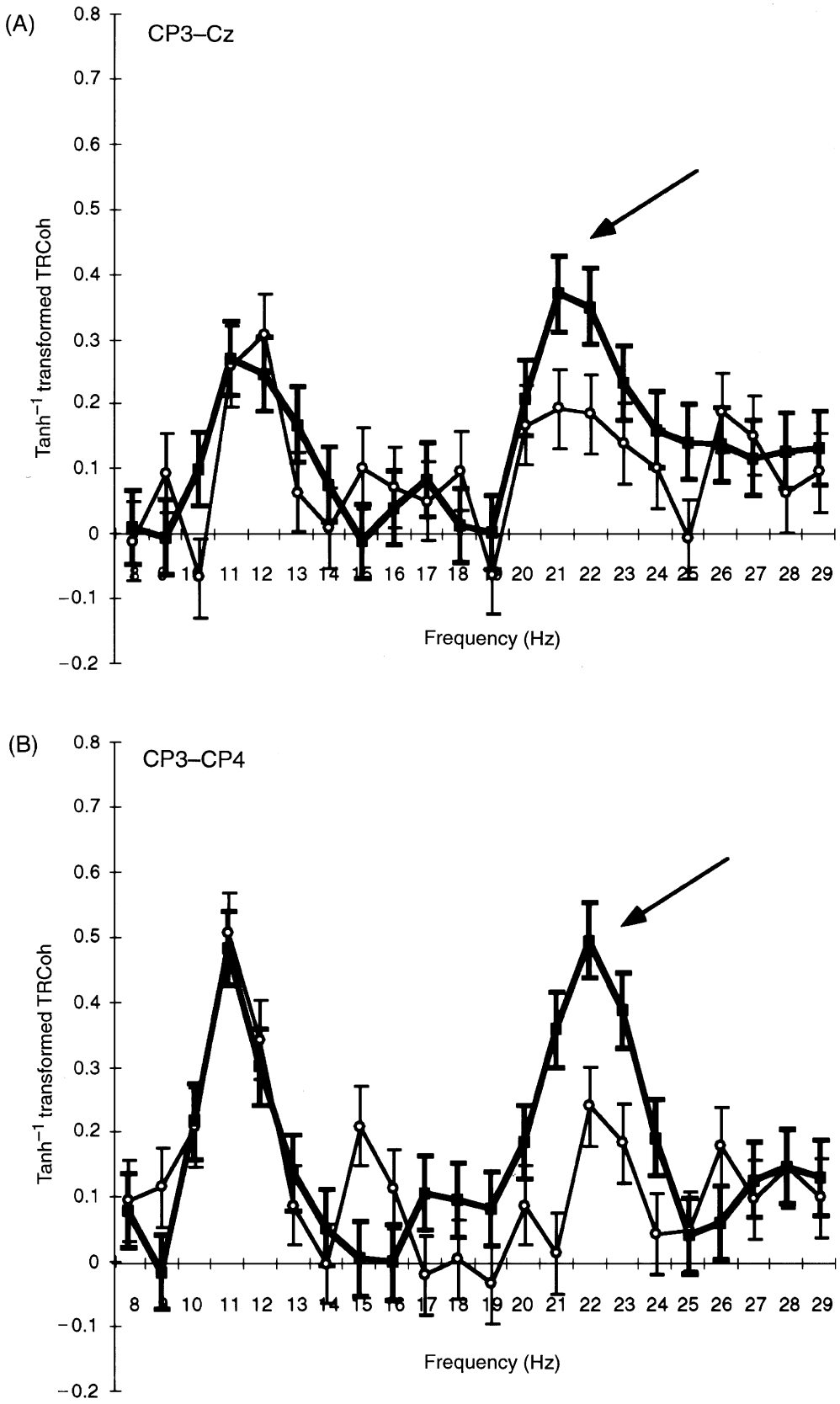

Fig. 8 Tanh^{-1}-transformed task-related coherence data for an individual subject. The task-related coherence is plotted as a function of frequency (in 1 Hz steps). (**A**) Electrode pair representing the connection between left central and mesial frontocentral cortex (including the SMA). (**B**) Electrode pair representing the connection between left and right central region (left and right premotor and primary sensorimotor cortex). Note the pronounced difference between internally paced (thick lines) and externally paced (thin lines) finger extensions in the β but not the α band (arrows). Error bars: ±3 SE.

Pfurtscheller, 1995, 1996). The precise relationship between task-related regional power decreases in the human EEG and in MEG and focal oscillatory short power increases ('bursts') in similar frequency ranges, as observed in local field potential recordings in non-human primates, has not yet been determined. One concept could be that, at rest, relatively widespread synchronized α and β oscillations reflect an idling state of the brain (Pfurtscheller *et al.*, 1996). Idling rhythms might be established in cortical networks or driven by a common thalamic pacemaker (Steriade and Amzica, 1996). From the aspect of information theory (e.g. Shannon and Weaver, 1949), in such an idling state the signal is highly predictable and the entropy is low, and the information content is therefore low. A task-related oscillatory burst in a circumscribed subset of neurons inside a cortical region could then occur out of synchrony with the idling rhythm but in the same frequency band. This burst would cause a local decrease of the spectral power in this frequency band (task-related power decrease). Disruption of the orderly idling rhythm would increase the entropy of the system and, thus, the information content. If, in this model, the burst were then synchronized with concomitant bursts in other activated areas, one would observe increased inter-regional coherence together with decreased power, as in the present study.

The maximal task-related power decreases in electrodes C3, CP3 and FC3 in the present study probably reflect the activation of the primary motor, primary sensory and probably lateral premotor cortex during internally paced and externally paced movements. Accordingly, the extension of the activated task-related power area towards electrodes FCz and Fz during internally paced movements would be most readily explained by additional activation of the mesial frontocentral cortex, particularly the SMA. This additional midline activation cannot be explained by a volume conduction artefact secondary to more pronounced bilateral task-related power decreases in both the lateral premotor and the sensorimotor area (Boetzel *et al.*, 1993), because the enhanced task-related power decrease over the ipsilateral central cortex was, although clearly present, too low in amplitude to extend to the midline via volume conduction (Fig. 5). Moreover, if volume conduction were the reason for additional task-related power decreases over the midline, then we would expect the mesial maximum to be in electrode Cz, not in FCz and Fz, where it occurred. The involvement of the contralateral sensorimotor and premotor cortex, of the SMA and, to a variable extent, of the ipsilateral lateral premotor cortex/SM1 in the generation of repetitive finger movements is in line with previous PET results (Orgogozo and Larsen, 1979; Roland *et al.*, 1980; Roland, 1984; Colebatch *et al.*, 1991; Deiber *et al.*, 1991; Shibasaki *et al.*, 1993; Kawashima *et al.*, 1994; Sadato *et al.*, 1996*a*, *b*) and fMRI (Kim *et al.*, 1993; Rao *et al.*, 1993; Boecker *et al.*, 1994; Karni *et al.*, 1995; Gerloff *et al.*, 1996).

The increased activation of the mesial frontocentral cortex corresponds well with the recent data of Deiber *et al*. (1996), who found that the anterior part of the SMA (pre-SMA) was more active during internally selected than during externally cued movements, and with observations in an earlier functional MRI study by Rao *et al.* (1993) showing more extended activation of cortical motor areas, including the SMA, when movements were internally rather than externally paced. An even more striking correspondence exists between the present data and invasive recordings in primates (Mushiake *et al.*, 1991; Halsband *et al.*, 1994), demonstrating that pre-SMA and SMA neurons exhibited a preferential relationship with internally generated movements. It has to be emphasized, however, that pre-SMA neurons also fired in association with the preparation of externally paced movements (Halsband *et al.*, 1994). It is therefore likely that the SMA is generally more involved in the generation of internally paced movements, but that its contribution is not restricted to this type of movement (Tanji and Shima, 1994, 1996; Shima *et al.*, 1996). This would be consistent with the model of a cortical motor network that modulates the balance of regional activation (in its network 'nodes') rather than actually 'switching' individual areas on or off. This concept is further supported by our coherence results.

Functional coupling versus regional activation in the cortical motor network: inter-regional coherence and regional oscillatory activity

The present coherence data suggest that the human cortical motor areas function in a network-like fashion and may use synchronization and desynchronization of oscillatory activity between distant regions in addition to increases and decreases in the magnitude of regional oscillatory activity.

Animal experiments have shown that inter-regional functional coupling, as determined by cross-correlation analysis of oscillatory activity in the time domain, is a potential mechanism for encoding behavioural parameters in the visual system over short and long distances (Engel *et al.*, 1991*a*, *b*; Singer, 1993, 1994; Fries *et al.*, 1996), in the auditory (deCharms and Merzenich, 1996) and olfactory (Laurent *et al.*, 1996) systems, in relation to motor behaviour (Murthy and Fetz, 1992; Sanes and Donoghue, 1993) and visuomotor integration (Bressler, 1995). Correlated activity in distant brain areas has also been observed in relation to visuomotor performance in humans, based on covariance analysis of time-averaged, bandpass-filtered (e.g. δ and θ bands: 0.1–3 Hz and 4–7 Hz) EEG potentials (Gevins *et al.*, 1987, 1989*a*, *b*, 1990), and based on coherence (task-related coherence) analysis of raw EEG signals in the frequency domain (Classen *et al*., 1998). In the present study, task-related coherence was focused over the central premotor and sensorimotor regions during both internally paced and externally paced movements, indicating that the coherence changes were topographically restricted. These regions (left and right central, mesial frontocentral) were covered by the POI that we used for statistical analysis. In addition to the POI (and without a clear correlate in the task-related power

topographic maps), there was a considerable number of links between left central, mesial frontocentral and right parietal regions during internally paced movements (β band). This suggests that coupling of the premotor and sensorimotor areas with the right parietal cortex is also relevant for this type of finger movement (particularly if internally paced). Similar involvement of the right parietal cortex (particularly Brodmann area 7) in unimanual, right-handed motor performance has been shown previously with PET (Deiber *et al.*, 1996).

The majority of previous results in animals suggest that enhanced functional coupling of cortical regions, as signified by increases in inter-regional cross-correlation, reflects excitatory interaction (Engel *et al.*, 1991*a*, *b*; Chiang *et al.*, 1996; Fries *et al.*, 1996; Roelfsema *et al.*, 1997). This is also a very plausible interpretation of the functional links between mesial premotor and lateral premotor and sensorimotor regions in our study. Yet task-related coherence increases cannot necessarily always be interpreted as excitatory. It is conceivable that inhibitory interneurons also contribute to systems that generate long-range synchronous oscillations (Jefferys *et al.*, 1996; Traub *et al.*, 1996). With respect to the present data, we favour the interpretation that the functional links between bilateral sensorimotor regions are inhibitory, at least in part. The structural basis for such inhibitory interhemispheric interactions could be transcallosal projections of GABAergic neurons to homologous areas (Jones, 1993). Their function may be to inhibit mirror movements. Based on EMG recordings from finger extensors of both forearms, we can exclude mirror movements of the left hand in the present study, thus indicating efficient interhemispheric inhibition on a behavioural level.

Interhemispheric, transcallosally mediated coherence would probably be an example of oscillatory activity that is synchronized via reciprocal corticocortical connections (Munk *et al.*, 1995; Lopes da Silva, 1996), as has also been suggested for the visual system (Engel *et al.*, 1991*a*; Singer, 1993, 1995) and the motor and sensory cortex (Murthy and Fetz, 1992). However, it is unclear whether this is always the mechanism that generates inter-regional coherence. An alternative explanation would be based on a common pacemaker (thalamus, reticular formation) (Lopes da Silva, 1996; Munk *et al.*, 1996). For example, thalamocortical interactions with relevance for the modulation of cortical oscillations have been described in detail for the occipital α rhythm (Contreras and Steriade, 1995, 1996; Steriade and Amzica, 1996; Steriade *et al.*, 1996*a*, *b*) and in the rat somatosensory cortex and VPL thalamus at 7–12 Hz and 19–21 Hz (Nicolelis *et al.*, 1995). The present investigation does not allow the differentiation of these candidate mechanisms. However, it seems likely that, depending on the regions involved, a combination of both mechanisms generates the large-scale coherence changes that can be measured in the human scalp-recorded EEG.

The observation that the maximal task-dependent coherence differences occurred in a frequency range (20–22 Hz) that did not show significant differences in regional activation (task-related power, maximum at 9–11 Hz) suggests that different frequencies may represent different functional aspects of information processing in this network of cortical motor regions. Different behaviour of oscillatory activity of task-related spectral power changes in the α and β bands has been reported in EEG and MEG studies (Tiihonen *et al.*, 1989; Nashmi *et al.*, 1994; Pfurtscheller *et al.*, 1994; Toro *et al.*, 1994*b*). Interestingly, coherent rhythmicity in the β range has also been demonstrated between motor cortical activity and EMG (Conway *et al.*, 1995; Baker *et al.*, 1997; Salenius *et al.*, 1997). It is therefore tempting to speculate that synchronous oscillations in the 20 Hz range may bind together the final common pathway of motoneuron activity with primary and premotor activity. The divergence between task-related coherence (20–22 Hz) and task-related power (9–11 Hz) (i.e. the fact that human cortical networks may accomplish different motor task demands by modulating inter-regional coupling even without obvious changes in regional activation) seems to be an additional novel and important finding of the present study that needs to be addressed systematically in future experiments.

Acknowledgements

The authors wish to thank Drs M. Honda and R. Weeks for their comments, and Ms B. J. Hessie for skilful editing. We would also like to thank the reviewers for their constructive comments and detailed discussion of the data and the statistical procedures. C.G. was supported by the Deutsche Forschungsgemeinschaft (Ge 844/1–1).

References

Amjad AM, Halliday DM, Rosenberg JR, Conway BA. An extended difference of coherence test for comparing and combining several independent coherence estimates: theory and application to the study of motor units and physiological tremor. J Neurosci Methods 1997; 73: 69–79.

Andrew C, Pfurtscheller G. Event-related coherence as a tool for studying dynamic interaction of brain regions. Electroencephalogr Clin Neurophysiol 1996; 98: 144–8.

Baker SN, Olivier E, Lemon RN. Coherent oscillations in monkey motor cortex and hand muscle EMG show task-dependent modulation. J Physiol (Lond) 1997; 501: 225–41.

Barrett G, Shibasaki H, Neshige R. Cortical potentials preceding voluntary movement: evidence for three periods of preparation in man. Electroencephalogr Clin Neurophysiol 1986; 63: 327–39.

Boecker H, Kleinschmidt A, Requardt M, Hanicke W, Merboldt KD, Frahm J. Functional cooperativity of human cortical motor areas during self-paced simple finger movements. A high-resolution MRI study. Brain 1994; 117: 1231–9.

Boetzel K, Plendl H, Paulus W, Scherg M. Bereitschaftspotential: is there a contribution of the supplementary motor area? Electroencephalogr Clin Neurophysiol 1993; 89: 187–96.

Bressler SL. Large-scale cortical networks and cognition. [Review]. Brain Res Brain Res Rev 1995; 20: 288–304.

Chatrian GE, Petersen MC, Lazarete JA. The blocking of the rolandic wicket rhythm and some central changes related to movement. Electroencephalogr Clin Neurophysiol 1959; 11: 497–510.

Chiang C, von Stein A, König P. Synchronous activity between primary visual and sensorimotor cortex in the awake behaving cat [abstract]. Soc Neurosci Abstr 1996; 22: 643.

Classen J, Gerloff C, Honda M, Hallett M. Integrative visuomotor behavior is associated with interregionally coherent oscillations in the human brain. J Neurophysiol 1998; 79: 1567–73.

Colebatch JG, Deiber MP, Passingham RE, Friston KJ, Frackowiak RSJ. Regional cerebral blood flow during voluntary arm and hand movements in human subjects. J Neurophysiol 1991; 65: 1392–401.

Contreras D, Steriade M. Cellular basis of EEG slow rhythms: a study of dynamic corticothalamic relationships. J Neurosci 1995; 15: 604–22.

Contreras D, Steriade M. Spindle oscillation in cats: the role of corticothalamic feedback in a thalamically generated rhythm [published erratum appears in J Physiol (Lond) 1996; 491: 889]. J Physiol (Lond) 1996; 490: 159–79.

Conway BA, Halliday DM, Farmer SF, Shahani U, Maas P, Weir AI, et al. Synchronization between motor cortex and spinal motoneuronal pool during the performance of a maintained motor task in man. J Physiol (Lond) 1995; 489: 917–24.

Cunnington R, Iansek R, Bradshaw JL, Phillips JG. Movement-related potentials in Parkinson's disease. Presence and predictability of temporal and spatial cues. Brain 1995; 118: 935–50.

deCharms RC, Merzenich MM. Primary cortical representation of sounds by the coordination of action-potential timing. Nature 1996; 381: 610–3.

Deecke L. Bereitschaftspotential as an indicator of movement preparation in supplementary motor area and motor cortex. Ciba Found Symp 1987; 132: 231–50.

Deecke L, Kornhuber HH. An electrical sign of participation of the mesial 'supplementary' motor cortex in human voluntary finger movement. Brain Res 1978; 159: 473–6.

Deecke L, Lang W, Heller HJ, Hufnagl M, Kornhuber HH. Bereitschaftspotential in patients with unilateral lesions of the supplementary motor area. J Neurol Neurosurg Psychiatry 1987; 50: 1430–4.

Deiber MP, Passingham RE, Colebatch JG, Friston KJ, Nixon PD, Frackowiak RS. Cortical areas and the selection of movement: a study with positron emission tomography. Exp Brain Res 1991; 84: 393–402.

Deiber MP, Ibanez V, Sadato N, Hallett M. Cerebral structures participating in motor preparation in humans—a positron emission tomography study. J Neurophysiol 1996; 75: 233–47.

Dick JP, Cantello R, Buruma O, Gioux M, Benecke R, Day BL, et al. The Bereitschaftspotential, L-DOPA and Parkinson's disease. Electroencephalogr Clin Neurophysiol 1987; 66: 263–74.

Dick JP, Rothwell JC, Day BL, Cantello R, Buruma O, Gioux M, et al. The Bereitschaftspotential is abnormal in Parkinson's disease. Brain 1989; 112: 233–44.

Engel AK, Konig P, Kreiter AK, Singer W. Interhemispheric synchronization of oscillatory neuronal responses in cat visual cortex. Science 1991a; 252: 1177–9.

Engel AK, Konig P, Singer W. Direct physiological evidence for scene segmentation by temporal coding. Proc Natl Acad Sci USA 1991b; 88: 9136–40.

Farmer SF, Bremner FD, Halliday DM, Rosenberg JR, Stephens JA. The frequency content of common synaptic inputs to motoneurones studied during voluntary isometric contraction in man. J Physiol (Lond) 1993; 470: 127–55.

Fein G, Raz J, Brown FF, Merrin EL. Common reference coherence data are confounded by power and phase effects. Electroencephalogr Clin Neurophysiol 1988; 69: 581–4.

Fries P, Roelfsema PR, Engel AK, König P, Singer W. Synchronized gamma frequency oscillations correlate with perception during binocular rivalry in awake squinting cats [abstract]. Soc Neurosci Abstr 1996; 22: 282.

Gastaut H, Terzian H, Gastaut Y. Etude d'une activité arceau electroencéphalographique méconnue: 'le rythme rolandique en arceau'. Marseille Med 1952; 89: 296–310.

Gerloff C, Grodd W, Altenmüller E, Kolb R, Nägele T, Klose U, et al. Coregistration of EEG and fMRI in a simple motor task. Hum Brain Mapp 1996; 4: 199–209.

Gerloff C, Toro C, Uenishi N, Cohen LG, Leocani L, Hallett M. Steady-state movement-related cortical potentials: a new approach to assessing cortical activity associated with fast repetitive finger movements. Electroencephalogr Clin Neurophysiol 1997; 102: 106–13.

Gevins AS, Cutillo BA, Morgan NH, Bressler SL, Illes J, White RM, et al. Event-related covariances of a bimanual visuomotor task. Electroencephalogr Clin Neurophysiol Suppl 1987; 40: 31–40.

Gevins AS, Bressler SL, Morgan NH, Cutillo BA, White RM, Greer DS, et al. Event-related covariances during a bimanual visuomotor task. I. Methods and analysis of stimulus- and response-locked data. Electroencephalogr Clin Neurophysiol 1989a; 74: 58–75.

Gevins AS, Cutillo BA, Bressler SL, Morgan NH, White RM, Illes J, et al. Event-related covariances during a bimanual visuomotor task. II. Preparation and feedback. Electroencephalogr Clin Neurophysiol 1989b; 74: 147–60.

Gevins AS, Bressler SL, Cutillo BA, Illes J, Miller JC, Stern J, et al. Effects of prolonged mental work on functional brain topography. Electroencephalogr Clin Neurophysiol 1990; 76: 339–50.

Hallett M. Clinical neurophysiology of akinesia. [Review]. Rev Neurol (Paris) 1990; 146: 585–90.

Hallett M, Toro C. Generation of movement-related potentials in the supplementary sensorimotor area. [Review]. Adv Neurol 1996; 70: 147–52.

Halliday DM, Rosenberg JR, Amjad AM, Breeze P, Conway BA, Farmer SF. A framework for the analysis of mixed time series/point process data—theory and application to the study of physiological

tremor, single motor unit discharges and electromyograms. [Review]. Prog Biophys Mol Biol 1995; 64: 237–78.

Halsband U, Ito N, Tanji J, Freund HJ. The role of premotor cortex and the supplementary motor area in the temporal control of movement in man. Brain 1993; 116: 243–66.

Halsband U, Matsuzaka Y, Tanji J. Neuronal activity in the primate supplementary, pre-supplementary and premotor cortex during externally and internally instructed sequential movements. Neurosci Res 1994; 20: 149–55.

Homan RW, Herman J, Purdy P. Cerebral location of international 10–20 system electrode placement. Electroencephalogr Clin Neurophysiol 1987; 66: 376–82.

Ikeda A, Lüders HO, Burgess RC, Shibasaki H. Movement-related potentials recorded from supplementary motor area and primary motor area. Role of supplementary motor area in voluntary movements. Brain 1992; 115: 1017–43.

Ikeda A, Lüders HO, Burgess RC, Shibasaki H. Movement-related potentials associated with single and repetitive movements recorded from human supplementary motor area. Electroencephalogr Clin Neurophysiol 1993; 89: 269–77.

Ikeda A, Lüders HO, Shibasaki H. Generation of contingent negative variation in the supplementary sensorimotor area. [Review]. Adv Neurol 1996; 70: 153–9.

Jahanshahi M, Jenkins IH, Brown RG, Marsden CD, Passingham RE, Brooks DJ. Self-initiated versus externally triggered movements. I. An investigation using measurement of regional cerebral blood flow with PET and movement-related potentials in normal and Parkinson's disease subjects [see comments]. Brain 1995; 118: 913–33. Comment in: Brain 1996; 119: 1045–8.

Jasper H, Penfield W. Electrocorticograms in man: effect of voluntary movements upon the electrical activity of the precentral gyrus. Arch Psychiat Nervkrankh 1949; 183: 163–74.

Jefferys JG, Traub RD, Whittington MA. Neuronal networks for induced '40 Hz' rhythms [see comments]. Trends Neurosci 1996; 19: 202–8. Comment in: Trends Neurosci 1996; 19: 468–70.

Jenkins IH, Fernandez W, Playford ED, Lees AJ, Frackowiak RS, Passingham RE, et al. Impaired activation of the supplementary motor area in Parkinson's disease is reversed when akinesia is treated with apomorphine. Ann Neurol 1992; 32: 749–57.

Jones EG. GABAergic neurons and their role in cortical plasticity in primates. [Review]. Cereb Cortex 1993; 3: 361–72.

Karni A, Meyer G, Jezzard P, Adams MM, Turner R, Ungerleider LG. Functional MRI evidence for adult motor cortex plasticity during motor skill learning. Nature 1995; 377: 155–8.

Kawashima R, Roland PE, O'Sullivan BT. Fields in human motor areas involved in preparation for reaching, actual reaching, and visuomotor learning: a positron emission tomography study. J Neurosci 1994; 14: 3462–74.

Kim SG, Ashe J, Hendrich K, Ellermann JM, Merkle H, Ugurbil K, et al. Functional magnetic resonance imaging of motor cortex: hemispheric asymmetry and handedness. Science 1993; 261: 615–7.

Knosche T, Praamstra P, Stegeman D, Peters M. Linear estimation discriminates midline sources and a motor cortex contribution to the readiness potential. Electroencephalogr Clin Neurophysiol 1996; 99: 183–90.

Kurata K, Wise SP. Premotor and supplementary motor cortex in rhesus monkeys: neuronal activity during externally- and internally-instructed motor tasks. Exp Brain Res 1988; 72: 237–48.

Lang W, Obrig H, Lindinger G, Cheyne D, Deecke L. Supplementary motor area activation while tapping bimanually different rhythms in musicians. Exp Brain Res 1990; 79: 504–14.

Lang W, Cheyne D, Kristeva R, Beisteiner R, Lindinger G, Deecke L. Three-dimensional localization of SMA activity preceding voluntary movement. A study of electric and magnetic fields in a patient with infarction of the right supplementary motor area. Exp Brain Res 1991; 87: 688–95.

Laurent G, Wehr M, Davidowitz H. Temporal representations of odors in an olfactory network. J Neurosci 1996; 16: 3837–47.

Lopes da Silva FH. Biophysical issues at the frontiers of the interpretation of EEG/MEG signals. [Review]. Electroencephalogr Clin Neurophysiol 1996; 45: 1–7.

Lopes da Silva FH, Vos JE, Mooibroek J, van Rotterdam A. Relative contributions of intracortical and thalamo-cortical processes in the generation of α rhythms, revealed by partial coherence analysis. Electroencephalogr Clin Neurophysiol 1980; 50: 449–56.

MacKinnon CD, Kapur S, Hussey D, Verrier MC, Houle S, Tatton WG. Contributions of the mesial frontal cortex to the premovement potentials associated with intermittent hand movements in humans. Hum Brain Mapp 1996; 4: 1–22.

Marsden CD. Slowness of movement in Parkinson's disease. [Review]. Mov Disord 1989; 4 Suppl 1: S26–37.

Marsden CD, Deecke L, Freund HJ, Hallett M, Passingham RE, Shibasaki H, et al. The functions of the supplementary motor area. Summary of a workshop. Adv Neurol 1996; 70: 477–87.

McCarthy G, Wood CC. Scalp distributions of event-related potentials: an ambiguity associated with analysis of variance models. Electroencephalogr Clin Neurophysiol 1985; 62: 203–8.

Munk MH, Nowak LG, Nelson JI, Bullier J. Structural basis of cortical synchronization. II. Effects of cortical lesions. J Neurophysiol 1995; 74: 2401–14.

Munk MH, Roelfsema PR, Konig P, Engel AK, Singer W. Role of reticular activation in the modulation of intracortical synchronization [see comments]. Science 1996; 272: 271–4. Comment in: Science 1996; 272: 225–6.

Murthy VN, Fetz EE. Coherent 25- to 35-Hz oscillations in the sensorimotor cortex of awake behaving monkeys. Proc Natl Acad Sci USA 1992; 89: 5670–4.

Mushiake H, Inase M, Tanji J. Neuronal activity in the primate premotor, supplementary, and precentral motor cortex during visually guided and internally determined sequential movements. J Neurophysiol 1991; 66: 705–18.

Nashmi R, Mendonca AJ, MacKay WA. EEG rhythms of the sensorimotor region during hand movements. Electroencephalogr Clin Neurophysiol 1994; 91: 456–67.

Nicolelis MA, Baccala LA, Lin RC, Chapin JK. Sensorimotor

encoding by synchronous neural ensemble activity at multiple levels of somatosensory system. Science 1995; 268: 1353–8.

Oldfield RC. The assessment and analysis of handedness: the Edinburgh inventory. Neuropsychologia 1971; 9: 97–113.

Orgogozo JM, Larsen B. Activation of the supplementary motor area during voluntary movement in man suggests it works as a supramotor area. Science 1979; 206: 847–50.

Papakostopoulos D, Crow HJ, Newton P. Spatiotemporal characteristics of intrinsic evoked and event related potentials in the human cortex. In: Pfurtscheller G, Buser P, Lopes da Silva F, editors. Rhythmic EEG activities and cortical functioning. Amsterdam: Elsevier/North Holland; 1980. p. 179–99.

Pfurtscheller G. Central beta rhythm during sensorimotor activities in man. Electroencephalogr Clin Neurophysiol 1981; 51: 253–64.

Pfurtscheller G. Mapping of event-related desynchronization and type of derivation. Electroencephalogr Clin Neurophysiol 1988; 70: 190–3.

Pfurtscheller G. Event-related synchronization (ERS): an electrophysiological correlate of cortical areas at rest. Electroencephalogr Clin Neurophysiol 1992; 83: 62–9.

Pfurtscheller G, Pregenzer M, Neuper C. Visualization of sensorimotor areas involved in preparation for hand movement based on classification of mu and central beta rhythms in single EEG trials in man. Neurosci Lett 1994; 181: 43–6.

Pfurtscheller G, Stancak A Jr, Neuper C. Event-related synchronization (ERS) in the α band—an electrophysiological correlate of cortical idling: a review. [Review]. Int J Psychophysiol 1996; 24: 39–46.

Picard N, Strick PL. Comparison of 2DG uptake in medial wall motor areas during performance of visually-guided and remembered sequences of movements [abstract]. Soc Neurosci Abstr 1996a; 22: 2025.

Picard N, Strick PL. Motor areas of the medial wall: a review of their location and functional activation. [Review]. Cereb Cortex 1996b; 6: 342–53.

Playford ED, Jenkins IH, Passingham RE, Nutt J, Frackowiak RS, Brooks DJ. Impaired mesial frontal and putamen activation in Parkinson's disease: a positron emission tomography study. Ann Neurol 1992; 32: 151–61.

Praamstra P, Cools AR, Stegeman DF, Horstink MW. Movement-related potential measures of different modes of movement selection in Parkinson's disease. J Neurol Sci 1996; 140: 67–74.

Rao SM, Binder JR, Bandettini PA, Hammeke TA, Yetkin FZ, Jesmanowicz A, et al. Functional magnetic resonance imaging of complex human movements. Neurology 1993; 43: 2311–8.

Rappelsberger P, Petsche H. Probability mapping: power and coherence analyses of cognitive processes. Brain Topogr 1988; 1: 46–54.

Rappelsberger P, Pfurtscheller G, Filz O. Calculation of event-related coherence—a new method to study short-lasting coupling between brain areas. Brain Topogr 1994; 7: 121–7.

Rascol O, Sabatini U, Chollet F, Celsis P, Montastruc JL, Marc-Vergnes JP, et al. Supplementary and primary sensory motor area activity in Parkinson's disease. Regional cerebral blood flow changes during finger movements and effects of apomorphine. Arch Neurol 1992; 49: 144–8.

Rascol OJ, Sabatini U, Chollet F, Montastruc JL, Marc-Vergnes JP, Rascol A. Impaired activity of the supplementary motor area in akinetic patients with Parkinson's disease. Improvement by the dopamine agonist apomorphine. Adv Neurol 1993; 60: 419–21.

Rascol O, Sabatini U, Chollet F, Fabre N, Senard JM, Montastruc JL, et al. Normal activation of the supplementary motor area in patients with Parkinson's disease undergoing long-term treatment with levodopa. J Neurol Neurosurg Psychiatry 1994; 57: 567–71.

Remy P, Zilbovicius M, Leroy-Willig A, Syrota A, Samson Y. Movement- and task-related activations of motor cortical areas: a positron emission tomographic study [see comments]. Ann Neurol 1994; 36: 19–26. Comment in: Ann Neurol 1995; 37: 282–4.

Roelfsema PR, Engel AK, Konig P, Singer W. Visuomotor integration is associated with zero time-lag synchronization among cortical areas. Nature 1997; 385: 157–61.

Roland PE. Organization of motor control by the normal human brain. Hum Neurobiol 1984; 2: 205–16.

Roland PE, Larsen B, Lassen NA, Skinhoj E. Supplementary motor area and other cortical areas in organization of voluntary movements in man. J Neurophysiol 1980; 43: 118–36.

Romo R, Schultz W. Role of primate basal ganglia and frontal cortex in the internal generation of movements. III. Neuronal activity in the supplementary motor area. Exp Brain Res 1992; 91: 396–407.

Rosenberg JR, Amjad AM, Breeze P, Brillinger DR, Halliday DM. The Fourier approach to the identification of functional coupling between neuronal spike trains: maximum likelihood analysis of spike trains of interacting nerve cells. [Review]. Prog Biophys Mol Biol 1989; 53: 1–31.

Sadato N, Campbell G, Ibanez V, Deiber MP, Hallett M. Complexity affects regional cerebral blood flow change during sequential finger movements. J Neurosci 1996a; 16: 2691–700.

Sadato N, Ibanez V, Deiber MP, Campbell G, Leonardo M, Hallett M. Frequency-dependent changes of regional cerebral blood flow during finger movements. J Cereb Blood Flow Metab 1996b; 16: 23–33.

Salenius S, Portin K, Kajola M, Salmelin R, Hari R. Cortical control of human motoneuron firing during isometric contraction. J Neurophysiol 1997; 77: 3401–5.

Salmelin R, Hari R. Spatiotemporal characteristics of sensorimotor neuromagnetic rhythms related to thumb movement. Neuroscience 1994; 60: 537–50.

Sanes JN, Donoghue JP. Oscillations in local field potentials of the primate motor cortex during voluntary movement. Proc Natl Acad Sci USA 1993; 90: 4470–4.

Schoppenhorst M, Brauer F, Freund G, Kubicki S. The significance of coherence estimates in determining central alpha and mu activities. Electroencephalogr Clin Neurophysiol 1980; 48: 25–33.

Shannon CE, Weaver W. The mathematical theory of communication. Urbana: University of Illinois Press; 1949.

Shaw JC. Correlation and coherence analysis of the EEG: a selective tutorial review. Int J Psychophysiol 1984; 1: 255–66.

Shibasaki H, Sadato N, Lyshkow H, Yonekura Y, Honda M, Nagamine T, et al. Both primary motor cortex and supplementary motor area play an important role in complex finger movement. Brain 1993; 116: 1387–98.

Shima K, Mushiake H, Saito N, Tanji J. Role for cells in the presupplementary motor area in updating motor plans. Proc Natl Acad Sci USA 1996; 93: 8694–8.

Singer W. Neuronal representations, assemblies and temporal coherence. [Review]. Prog Brain Res 1993; 95: 461–74.

Singer W. Coherence as an organizing principle of cortical functions. [Review]. Int Rev Neurobiol 1994; 37: 153–83; discussion 203–7.

Singer W. Development and plasticity of cortical processing architectures. [Review]. Science 1995; 270: 758–64.

Stancak A Jr, Pfurtscheller G. The effects of handedness and type of movement on the contralateral preponderance of mu-rhythm desynchronization. Electroencephalogr Clin Neurophysiol 1996; 99: 174–82.

Stancak A Jr, Pfurtscheller G. Desynchronization and recovery of beta rhythms during brisk and slow self-paced finger movements in man. Neurosci Lett 1995; 196: 21–4.

Steinmetz H, Fuerst G, Meyer B-U. Craniocerebral topography within the international 10–20 system. Electroencephalogr Clin Neurophysiol 1989; 72: 499–506.

Steriade M, Amzica F. Intracortical and corticothalamic coherency of fast spontaneous oscillations. Proc Natl Acad Sci USA 1996; 93: 2533–8.

Steriade M, Amzica F, Contreras D. Synchronization of fast (30–40 Hz) spontaneous cortical rhythms during brain activation. J Neurosci 1996a; 16: 392–417.

Steriade M, Contreras D, Amzica F, Timofeev I. Synchronization of fast (30–40 Hz) spontaneous oscillations in intrathalamic and thalamocortical networks. J Neurosci 1996b; 16: 2788–808.

Tanji J. The supplementary motor area in the cerebral cortex. [Review]. Neurosci Res 1994; 19: 251–68.

Tanji J, Shima K. Role for supplementary motor area cells in planning several movements ahead. Nature 1994; 371: 413–6.

Tanji J, Shima K. Supplementary motor cortex in organization of movement. [Review]. Eur Neurol 1996; 36 Suppl 1: 13–9.

Thatcher RW. Tomographic electroencephalography/ magnetoencephalography. Dynamics of human neural network switching. [Review]. J Neuroimaging 1995; 5: 35–45.

Tiihonen J, Kajola M, Hari R. Magnetic mu rhythm in man. Neuroscience 1989; 32: 793–800.

Toro C, Matsumoto J, Deuschl G, Roth BJ, Hallett M. Source analysis of scalp-recorded movement-related electrical potentials. Electroencephalogr Clin Neurophysiol 1993; 86: 167–75.

Toro C, Cox C, Friehs G, Ojakangas C, Maxwell R, Gates JR, et al. 8–12 Hz rhythmic oscillations in human motor cortex during two-dimensional arm movements: evidence for representation of kinematic parameters. Electroencephalogr Clin Neurophysiol 1994a; 93: 390–403.

Toro C, Deuschl G, Thatcher R, Sato S, Kufta C, Hallett M. Event-related desynchronization and movement-related cortical potentials on the ECoG and EEG. Electroencephalogr Clin Neurophysiol 1994b; 93: 380–9.

Traub RD, Whittington MA, Stanford IM, Jefferys JG. A mechanism for generation of long-range synchronous fast oscillations in the cortex. Nature 1996; 383: 621–4.

Weiss S, Rappelsberger P. EEG coherence within the 13–18 Hz band as a correlate of a distinct lexical organisation of concrete and abstract nouns in humans. Neurosci Lett 1996; 209: 17–20.

Wessel K, Zeffiro T, Toro C, Hallett M. Self-paced versus metronome-paced finger movements: a positron emission tomography study. J Neuroimaging 1997; 7: 145–151.

Received January 14, 1998. Revised April 2, 1998.
Accepted April 4, 1998